ACS OMEGA

http://pubs.acs.org/journal/acsodf

Article

Observation of Arginine Side-Chain Motions Coupled to the Global Conformational Exchange Process in Deubiquitinase A

Ashish Kabra, Efsita Rumpa, and Ying Li*

Cite This: *ACS Omega* 2022, 7, 9936−9943

Read Online

ACCESS | Metrics & More | Article Recommendations | Supporting Information

ABSTRACT: Coupled motions have been demonstrated to be functionally important in a number of enzymes. Noncovalent side-chain interactions play essential roles in coordinating the motions across different structural elements in a protein. However, most of the dynamic studies of proteins are focused on backbone amides or methyl groups in the side chains and little is known about the polar and charged side chains. We have previously characterized the conformational dynamics of deubiquitinase A (DUBA), an isopeptidase, on the microsecond-to-millisecond (μs−ms) time scales with the amide ^{1}H Carr−Purcell−Meiboom−Gill (CPMG) experiment. We detected a global conformational exchange process on a time scale of approximately 200 μs, which involves most of the structural elements in DUBA, including the active site and the substrate binding interface. Here, we extend our previous study on backbone amides to the arginine side-chain N$^\epsilon$−H$^\epsilon$ groups using a modified ^{1}H CPMG pulse sequence that can efficiently detect both backbone amide and arginine side-chain N$^\epsilon$−H$^\epsilon$ signals in a single experiment. We found that the side chains of three arginines display motions on the same time scale as the backbone amides. Mutations of two of the three arginines to alanines result in a decrease in enzyme activity. One of these two arginines is located in a loop involved in substrate binding. This loop is not visible in the backbone amide-detected experiments due to excess line broadening induced by motions on the μs−ms time scales. These results clearly demonstrate that the motions of some arginine side chains are coupled to the global conformational exchange process and provide an additional probe for motions in a functionally important loop that did not yield visible backbone amide signals, suggesting the value of side-chain experiments on DUBA. The modified ^{1}H CPMG pulse sequence allows the simultaneous characterization of backbone and arginine side-chain dynamics without any increase in data acquisition time and can be applied to the dynamic studies of any protein that displays measurable amide ^{1}H relaxation dispersion.

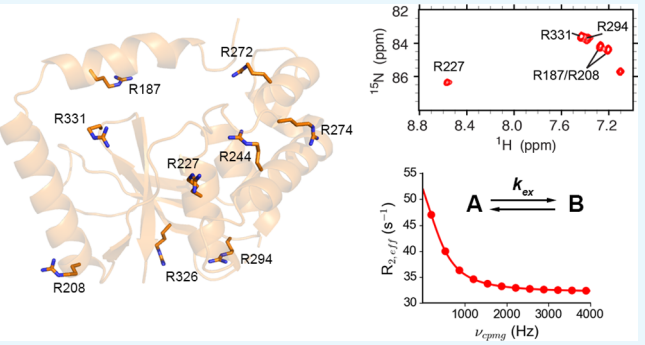

INTRODUCTION

Deubiquitinase A (DUBA), also named OTUD5, is a member of the deubiquitinase (DUB) family, which consists of ∼100 members in humans.[1] Deubiquitinases (DUBs) are involved in most of the biological processes in eukaryotes through deconjugation of single ubiquitin molecules or polyubiquitin chains from target proteins.[2] Polyubiquitin chains can form from linking the C-terminus of one ubiquitin to one of the seven lysines (K6, K11, K27, K29, K33, K48, K63) or the N-terminal methionine of another ubiquitin. Ubiquitin chains formed via different linkages represent distinct physiological signals.[3] Removal of ubiquitin moieties by DUBs can result in changes in the stability, activity, subcellular locations, or interaction specificity of target proteins.[4] DUBA was initially identified as a negative regulator of type I interferons from siRNA screening.[5] It was subsequently found to be involved in other important biological processes, including cytokine production in T cells[6] and dendritic cells,[7] human development,[8] DNA damage response,[9] and tumorigenesis.[10] The activity of DUBA is regulated by phosphorylation at a single site, S177.[11] In biochemical assays *in vitro*, DUBA cleaves K48- and K63-linked polyubiquitin chains, though weak activity was also detected for K11-linked chains.[11,12]

DUBs are tightly regulated through a variety of mechanisms, including the abundance, subcellular localization, posttranslational modifications (PTMs), and binding of accessory domains to the catalytic domain.[4,13] Misregulation and loss of function of DUBs have been associated with human diseases.[14] In recent years, DUBs have become emerging therapeutic targets for treating cancer, inflammation, and neurodegenerative diseases. Development of selective DUB inhibitors has attracted interest from both academia and

Received: January 24, 2022
Accepted: February 25, 2022
Published: March 8, 2022

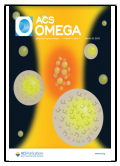

https://doi.org/10.1021/acsomega.2c00492
ACS Omega 2022, 7, 9936−9943

industry.[15] The molecular basis of DUB regulation and substrate specificity has been the subject of many biochemical and structural studies.[4,13] Many of these studies have implied the functional importance of conformational dynamics in the DUB family but the exact functional roles are not well understood for most DUBs. Conformational remodeling of DUBs by substrates, partner proteins, accessory domains, and PTMs was thought to be essential for the regulation and substrate specificity of many DUBs, but the detailed mechanisms are only known in a few cases.[16−19]

We have recently characterized the backbone dynamics of DUBA on the sub-millisecond time scales, using nuclear magnetic resonance (NMR) relaxation dispersion experiments.[20] We observed that most of the structural elements in DUBA are involved in a global conformational exchange process on a time scale of ∼200 μs. Notably, this process was detected on the phosphorylated S177 (pS177) in only one of the two conformers resolved by differences in the amide chemical shifts. The fact that this conformer is essential for DUBA activity suggests the functional importance of the observed global conformational process.[21] Mutations of two positively charged residues in the α6 helix, R272 and K273, to two glutamic acids lead to the decoupling of motions across different structural elements.[20] The observed decoupling suggests the loss of correlated motions if the similar exchange rate constants across many residues in the wild-type DUBA result from the coordination of different structural elements during conformational transition rather than a coincidence. According to the crystal structure of phosphorylated DUBA (p-DUBA) conjugated to ubiquitin aldehyde,[11] the mutations abolish the interactions between these two positively charged residues and the phosphate group in pS177 (Figure 1). In addition, two salt bridges between the α6 helix and the two neighboring structural elements, α5−α6 loop and α7 helix, were disrupted (Figure 1). The changes in the dynamic properties observed on the R272E/K273E mutant suggest that at least some salt bridges are essential for maintaining the global conformational process in DUBA. In this study, we set out to directly assess whether the motions of arginine side chains are coupled to this global process by quantifying the dynamics of these side chains with NMR relaxation dispersion experiments. We modified the pulse sequence for the backbone amide ^{1}H Carr−Purcell−Meiboom−Gill (CPMG) experiment used in our previous study[20] to enable the simultaneous detection of backbone amide and the arginine side-chain N^{ε}−H^{ε} without significant signal loss from the off-resonance effects. We were able to detect six out of a total of nine arginine N^{ε}−H^{ε} groups in the catalytic domain of DUBA at neutral pH and low temperature. We show that at least three arginine side chains undergo motions on the same time scale as a large number of backbone amides. Mutations of two of these three arginines to alanines result in partial loss of DUBA activity. Overall, our study provides spectroscopic evidence for the role of arginine side chains in coordinating the global conformational exchange process in DUBA on the sub-millisecond time scale and a rationale for further investigation of this role.

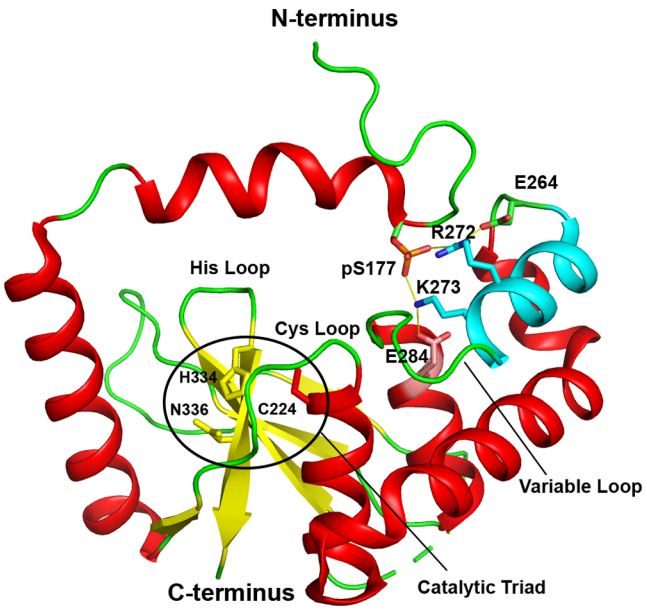

Figure 1. Crystal structure of DUBA (PDB code: 3TMP) with the α6 helix colored in cyan.

MATERIALS AND METHODS

NMR Sample Preparation and Conditions. The samples of U-[^{2}H,^{15}N] wild-type DUBA and U-^{15}N DUBA mutants were prepared according to previously reported methods.[22] The NMR sample buffer contains 50 mM sodium phosphate, pH 7.0, 100 mM NaCl, 1 mM Tris(2-carboxyethyl)phosphine (TCEP), 7% (v/v) D_2O, and 0.2 mM 4,4-dimethyl-4-silapentane-1-sulfonic acid (DSS).

^{1}H CPMG Experiment and Data Analysis. Amide ^{1}H CPMG experiments were performed on a 600 μM U-[^{2}H, ^{15}N] phosphorylated DUBA sample at 700 MHz ^{1}H frequency and 290 K, using the pulse sequence depicted in Figure 3. The Varian spectrometer used for the experiments is equipped with a cryoprobe. Each two-dimensional (2D) spectrum was acquired with 336 complex points and a spectral width of 3780 Hz (54 ppm) in the F1 (^{15}N) dimension. ^{15}N carrier was set at 120 ppm. The length of the CPMG period (T_{relax}) was 30 ms. A series of 2D spectra were acquired by varying the numbers of π refocusing pulses during the CPMG period, which were 0, 4, 8, 16 (replicated), 24, 32, 40, 48, 56, 64, 72, 80, 88, and 96. The data were acquired in an interleaved fashion. Twenty scans were accumulated with a recycle delay of 1.5 s, and the total data acquisition time was approximately 70 h.

The data were processed using NMRPipe[23] and visualized using Sparky.[24] The data analysis was performed as previously reported.[20] Briefly, the transverse relaxation rates ($R_{2,eff}$) were determined using cross-peak volumes measured without and with the constant-time relaxation period. Cross-peak volumes were determined using the program PINT.[25,26] The relaxation dispersion profiles were fit to a two-site exchange model under fast-exchange approximation[27]

$$R_{2,\mathrm{eff}} = \frac{\phi_{ex}}{k_{ex}}\left[1 - \frac{4\upsilon_{CPMG}}{k_{ex}}\tanh\left(\frac{k_{ex}}{4\upsilon_{CPMG}}\right)\right] + R_2^{o}$$

in which R_2^o is the limiting relaxation rate constant in the absence of exchange broadening; $\phi_{ex} = p_1p_2\Delta\omega_{12}^2$, where $\Delta\omega_{12}$ is the chemical shift difference between the two states, and p_1 and p_2 are the fractional populations of the two states, respectively; and $k_{ex} = k_1 + k_{-1}$, where k_1 and k_{-1} are the rate constants of the forward and reverse conformational transitions, respectively. The rate of transverse relaxation

https://doi.org/10.1021/acsomega.2c00492
ACS Omega 2022, 7, 9936−9943

resulting from the conformational exchange (R_{ex}) at $\nu_{CPMG} = 0$ was calculated according to $R_{ex} = \frac{p_1 p_2 \Delta\omega_{12}^2}{k_{ex}}$.

Ubiquitin−AMC Cleavage Assays. The single-turnover kinetic assays were performed, as previously described.[21] All samples were uniformly ^{15}N-labeled and prepared, as previously described.[22] The assays were performed at 25 °C in a buffer containing 50 mM HEPES, pH 7.5, 5 mM DTT, and 100 mM NaCl. The increase in the fluorescence intensity of 7-amino-4-methylcoumarin (AMC) when it is cleaved from ubiquitin was monitored using the SpectraMax Gemini XPS plate reader (Molecular Devices). The data were recorded until the reaction was at least 95% complete. The kinetic rate constant, k_2, and the substrate affinity, K_d, were determined from the recorded time courses, as previously described.[21] The assays were performed in duplicate on each DUBA mutant.

RESULTS

Assignment of Arginine Side-Chain N$^{\varepsilon}$−H$^{\varepsilon}$ Resonances. There are nine arginines in the catalytic domain of DUBA (Figure 2A), among which only six arginines (R187, R208, R227, R244, R294, and R326) yield visible backbone amide signals.[20] Six cross-peaks from the N$^{\varepsilon}$−H$^{\varepsilon}$ moiety of arginine side chains can be observed in the 2D ^{15}N HSQC spectrum, with ^{15}N carrier centered at 86 ppm and acquired at 290 K (Figure 2B). At higher temperatures, two cross-peaks (R187 and R208) become significantly weaker due to fast solvent exchange rates (data not shown). Despite the medium size (~20 kDa) of the catalytic domain of DUBA, it is a challenging system for obtaining reliable resonance assignments. Almost all of the backbone amide ^{1}H spectral lines are broadened due to conformational exchange on the μs−ms time scales. Approximately 30% of amide cross-peaks are not visible in the 2D ^{15}N TROSY spectrum. Although the 3D HNCACB experiment that correlates the C$^{\gamma}$ and C$^{\delta}$ with N$^{\varepsilon}$−H$^{\varepsilon}$ in the arginine side chain can, in principle, be employed to assign N$^{\varepsilon}$−H$^{\varepsilon}$ cross-peaks, the degeneracy of C$^{\gamma}$ and C$^{\delta}$ chemical shifts and the low sensitivity of 3D experiments for side-chain assignment make this method ineffective. Only R187 and R208 side chains are visible in this experiment but neither can be assigned unambiguously due to similar C$^{\gamma}$ and C$^{\delta}$ chemical shifts for these two residues. We have assigned three of the four remaining arginine side chains using three mutants, R227A, R294A, and R331A (Figure 2B). The remaining cross-peak was not assigned because μs−ms dynamics were not detected on this peak. Notably, the backbone amide of R331 is not visible but the side-chain N$^{\varepsilon}$−H$^{\varepsilon}$ can be detected with good sensitivity.

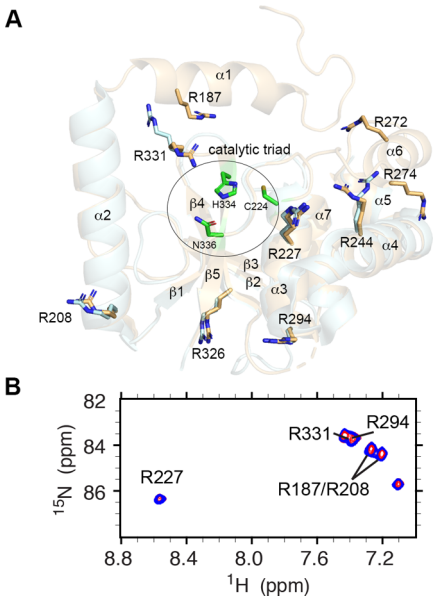

Figure 2. (A) Crystal structures of DUBA in the free form (cyan, PDB code: 3PFY) and of DUBA attached to ubiquitin aldehyde (gold, PDB code: 3TMP). (B) The ^{15}N HSQC spectra of arginine N$^{\varepsilon}$−H$^{\varepsilon}$ groups in wild-type phosphorylated (red) and nonphosphorylated (blue) DUBA.

Amide ^{1}H CPMG Experiment Using Broadband ^{15}N π Pulses. Amide ^{1}H CPMG experiment is an effective method for the characterization of conformational exchange on the μs−ms time scales. The chemical shifts of N$^{\varepsilon}$ in the guanidium group are typically in the range of 80−90 ppm, a few kilohertz away from the backbone amides, which resonate between 100 and 140 ppm. The hard π pulses used for the ^{15}N channel on a Cryoprobe are typically not short enough to fully invert or refocus the N$^{\varepsilon}$ magnetization when the ^{15}N carrier is centered on the amide at ~120 ppm. It has been demonstrated that replacing the hard ^{15}N π pulses with the broadband V1 pulse developed by Abramovich and Vega[28] allows the detection of arginine N$^{\varepsilon}$−H$^{\varepsilon}$ moiety with minimal signal loss in the context of the 3D HNCACB experiment for assigning arginine N$^{\varepsilon}$−H$^{\varepsilon}$ groups.[29] We have adopted this strategy and replaced the four hard ^{15}N π pulses in the original ^{1}H CPMG pulse sequence[30] with the V1 pulses. The modified pulse sequence is shown in Figure 3. The modified pulse sequence on average yielded improvement in signal intensity for N$^{\varepsilon}$−H$^{\varepsilon}$ cross-peaks by a factor of ~1.8 when the ^{15}N hard π/2 pulse length is 47.5 μs at 700 MHz ^{1}H frequency. The level of enhancement is very similar to that observed in the previous study.[29] Backbone signal loss due to the broadband pulses, which lead to shorter effective INEPT transfer periods, is negligible. The intensities of 67 backbone amide signals are on average 98% of those obtained using the original pulse sequence.

Microsecond-to-Millisecond Motions of Arginine Side Chains Characterized by Amide ^{1}H CPMG Experiments. We have previously measured the backbone amide ^{1}H relaxation dispersion on DUBA in both phosphorylated and nonphosphorylated forms at 298 K.[20] Here, we measured ^{1}H relaxation dispersion of both backbone amide and arginine side-chain N$^{\varepsilon}$−H$^{\varepsilon}$ on phosphorylated DUBA at 290 K. The lower sample temperature was chosen to reduce the signal loss from solvent exchange. R227, R294, and R331 display measurable ^{1}H$^{\varepsilon}$ relaxation dispersion (Figure 4A). Fitting data from these three residues individually yielded exchange rates (k_{ex}) of ~3000 s^{-1}. Group fitting was therefore performed, which yielded k_{ex} of 2580 ± 370 s^{-1}. Table 1 contains the dynamic parameters determined from the relaxation dispersion profiles. Global fitting was also performed across ~60 backbone amide resonances, as previously described.[20] The k_{ex} was 3230 ± 80 s^{-1}. The similar exchange rates of the arginine side chains and the many backbone amides indicate that motions of these side chains are coupled to the global conformational process. By contrast, the N$^{\varepsilon}$−H$^{\varepsilon}$ groups of R187 and R208 do not display measurable relaxation dispersion. In the crystal structure of DUBA, R331 and R227 form salt bridges with acidic side chains (Figure 4B and Table S1). R294 forms a H-bond with the backbone oxygen atom of

https://doi.org/10.1021/acsomega.2c00492
ACS Omega 2022, 7, 9936−9943

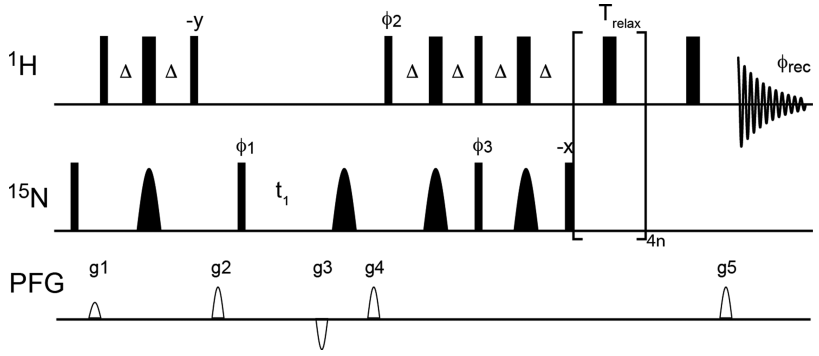

Figure 3. Pulse sequence diagram of the modified transverse relaxation optimized spectroscopy (TROSY)-selected ^{1}H CPMG experiment. The wide and narrow bars represent rectangular π pulse and $\pi/2$ pulses, respectively. The shaped pulses are 1.2 ms V1 pulses at a B_1 field of 5 kHz. All pulse phases are x unless indicated otherwise. Δ = 2.7 ms. The XY-16 phase alternating scheme ($x, y, x, y, y, x, y, x, -x, -y, -x, -y, -y, -x, -y, -x$) was used for the π pulse train during the T_{relax} period. n can be any integer. The phase cycle was $\phi1 = (-y, y)$, $\phi2 = y$, $\phi3 = y$, $\phi_{rec} = (-x, x)$. Quadrature detection in the indirect dimension was achieved by inverting $\phi2$ and $\phi3$ together with gradients g3 and g4 for every t_1 increment. The phase cycle is for Varian spectrometers. For Bruker spectrometers, y and $-y$ phases should be swapped. ^{1}H carrier was placed at 4.7 ppm for the entire pulse sequence except for the detection period. Gradients along the z axis have sine amplitude profiles, with peak strengths and durations as follows: g1 = 12.5 G/cm, 1.5 ms; g2 = 32.5 G/cm, 3 ms; g5 = 30 G/cm, 0.18 ms; g3 = −1.2 × g5, 0.9 ms; and g4 = 0.8 × g5, 0.9 ms.

E323, whereas R187 and R208 do not form H-bonds and are largely exposed to the solvent. The relaxation dispersion profiles of the backbone amide ^{1}H can be quantified for R187 and R208 at both 290 K (Figure 4A) and 298 K.[20] Flat relaxation dispersion profiles of side-chain H^{ε} can indicate the lack of side-chain motions for these two residues or that the motions are too fast to yield measurable relaxation dispersion. In the latter case, the backbone and side-chain motions are decoupled. For the three residues showing relaxation dispersion, the changes in the $^{1}H^{\varepsilon}$ chemical shifts likely result from changes in the ensemble-averaged configurations of salt bridges or H-bonds, which can propagate conformational changes to remote sites and enhance the coordination of motions across the entire protein.

Assessment of the Functional Importance of Arginines by Activity Assays. To assess the functional importance of arginines for which motions were detected, we performed activity assays on the R227A, R331A, and R294A mutants of phosphorylated DUBA, using the ubiquitin (Ub)−AMC substrate, where the fluorescent dye AMC was attached to the C-terminus of ubiquitin and can be cleaved by DUBs. Table 2 contains the kinetics parameters. R331A mutant shows a significantly lower catalytic rate constant despite the increased substrate affinity. R331 is located in a loop, named His loop, which precedes the β4 strand that contains the catalytic residue H334 (Figure 1). This loop is involved in substrate binding and was suggested by previous studies on other DUBs to control the substrate specificity.[12] By contrast, the R227A mutant has a very similar substrate affinity but the catalytic rate constant is lowered by 3-fold. The R294A mutant has the same substrate affinity and the catalytic rate constant as the wild type. The data suggest that a subset of arginine side chains involved in the global conformational exchange process are functionally important.

DISCUSSION

DUBA is a highly dynamic enzyme with coupled motions detected on the μs−ms time scales across most parts of the protein.[20] Coupled motions have been observed in enzymes in a number of families, including kinase[31] and phosphatase[32−34] and several model enzymes extensively studied by NMR and computational methods.[35] Although it is well understood that μs−ms motions play important roles in enzyme functions,[36,37] structural determinants of dynamic properties, especially those of correlated motions, are not well defined, which pose a significant challenge for the rational design of enzymes.[38] A recent study on a phosphatase, PTP1B, showed that small perturbations on weak interactions can significantly alter the dynamics of a functionally important loop and in turn the function of the enzyme.[33] Similarly, our previous study showed that the global conformational process in DUBA can be strongly perturbed by breaking only two salt bridges involving R272 and K273 (Figure 1) through mutations.[20] In the R272E/K273E mutant, many residues show elevated and highly variable kinetic rate constants, including those remote from the site of mutations. This observation suggests that an intact H-bond network may be essential for maintaining the dynamic property of wild-type DUBA and the rate constants of conformational exchange are highly sensitive to point mutations that disrupt the network. To further understand the role of the H-bond network for defining DUBA dynamics, we carried out this study to characterize the dynamic properties of arginine side chains, which are involved in the formation of salt bridges and hydrogen bonds.

The role of arginines in maintaining protein structural folds and stability has been widely investigated.[39] Arginine has a long and usually flexible side chain and contains five H-bond donors. Despite the importance of arginine for the structure, dynamics, and function of proteins, few NMR studies on arginine side-chain dynamics are available.[40−43] In recent years, sophisticated NMR methods have been developed to detect arginine side-chain signals with improved sensitivity and resolution.[44,45] Here, we assess whether the motions of arginine side chains are coupled to the global conformational process in DUBA, using a modified pulse sequence for the amide ^{1}H CPMG experiments. As expected, the three arginine side chains that display sub-millisecond motions all form salt bridges or H-bonds, among which the R331−E220 salt bridge connects two functionally important loops, the His loop (residues 331−333) and the Cys loop (residues 217−223) (Figure 4B), which are not close in the primary sequence. All DUBs in the ovarian tumor (OTU) subfamily, to which DUBA belongs, contain three functionally important loops, the His, Cys, and the variable (residues 274−281) loops (Figure 1).

https://doi.org/10.1021/acsomega.2c00492
ACS Omega 2022, 7, 9936−9943

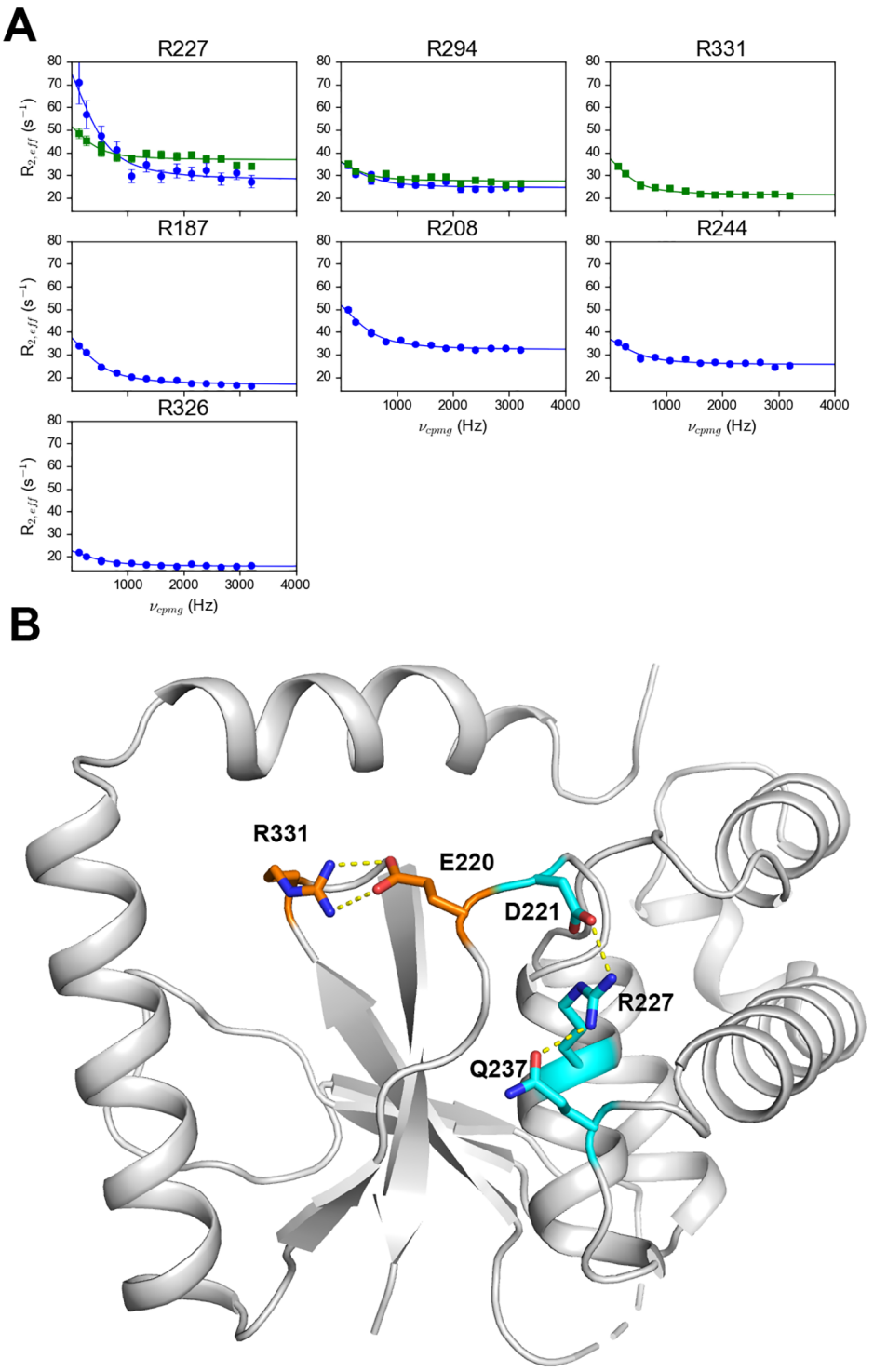

Figure 4. (A) Backbone amide ^{1}H (blue) and side-chain $^{1}H^{\epsilon}$ (green) relaxation dispersion profiles of arginine residues in DUBA. The side-chain data on R187 and R208 were not shown because the resonance assignment is ambiguous and neither residue displayed relaxation dispersion. The data were acquired at 700 MHz ^{1}H frequency and 290 K. (B) The crystal structure of DUBA (PDB code: 3TMP) with the salt bridges and H-bonds formed from R227 and R331 highlighted in stick representation.

The Cys loop in Cezanne, an OTU DUB, displays conformational plasticity and can shift from an inactive to active conformation upon substrate binding.[19] Variable loop and His loop are at the substrate binding interface and their amino acid sequences are highly variable across the OTU family, suggesting potential roles for controlling the linkage specificity of polyubiquitin substrates because OTU DUBs display distinct specificity despite the similar overall structural folds.[12] We have previously shown that two out of the three functionally important loops, Cys loop and the variable loop, undergo motions on the same time scale.[20] This study enabled the detection of a residue, R331, in the remaining loop, the His loop, which was not visible in the backbone amide-detected experiments.[20] R331 displays motions on the same time scale

https://doi.org/10.1021/acsomega.2c00492
ACS Omega 2022, 7, 9936−9943

Table 1. Group Fits of $^1H^\epsilon$ R_2 Relaxation Dispersion Curves of p-DUBA

name	R_{ex} (s^{-1})	$\phi_{ex}^{1/2}$(ppm)	k_{ex} (s^{-1})
R227	14.8 ± 0.5	0.045 ± 0.003	2580 ± 370
R294	8.7 ± 0.4	0.034 ± 0.003	
R331	16.0 ± 0.5	0.046 ± 0.003	

Table 2. Single-Turnover Kinetics of DUBA with Ub−AMC as the Substrate

enzyme	K_d (μM)	k_2 (10^{-3} s^{-1})
wild type[a]	31 ± 2	83 ± 1.5
R227A	43 ± 4	26 ± 1
R331A	8 ± 1	11 ± 0.2
R294A	28 ± 3	83 ± 2

[a]Wild-type data have been reported previously.[21]

as the entire DUBA molecule. Although the catalytic cysteine, C224, has been so far undetectable, it likely undergoes motions on the same time scale as many other structural elements, including the three loops, given the fact that many neighboring residues display such motions.[20] Overall, the data presented here and in our previous study[20] suggest that the motions of the catalytic cysteine and the three functionally important loops are coupled in DUBA. A recent NMR dynamic study on PTP1B, a phosphatase, made a similar observation that four catalytically important loops in this enzyme move as one dynamic unit.[34] R227, in the α3 helix, forms a H-bond with D221 in the Cys loop and Q237 in the α3−α4 loop (Figure 4B). The nearly unaltered substrate affinity and the significant change in the catalytic rate constant of the R227A mutant suggest a mostly intact substrate binding interface. The lower catalytic rate constant may result from the perturbation of the dynamic properties and/or the electrostatic environment of the active site because R227 is spatially close to the active site cysteine, C224. The remaining arginine displaying sub-millisecond motions in this study, R294, is also located in a loop, the α7−β2 loop. R294 side chain is H-bonded with the backbone oxygen atom of E323. However, the R294A mutant displays essentially unalerted enzyme kinetics, consistent with the expectation that this loop is not functionally important. Although the effects of the mutation can be long range, it appears that at least functionally important dynamic properties of DUBA are not perturbed. This mutant may serve as a negative control in future studies to distinguish between motions essential and nonessential for function. The two solvent-exposed arginines, R187 and R208 (Figure 2A), do not form H-bonds and show flat relaxation dispersion profiles. Overall, the dynamic data on arginine suggest that salt bridges or H-bonds are necessary for the arginine side-chain motions to be coupled to the global conformational exchange process on the μs−ms time scales.

The arginine side-chain data presented here are complementary to the previously reported backbone data on the R272E/K273E mutant,[20] both supporting the view that the H-bond network is essential for maintaining the global conformational exchange process involving many residues. Future studies on additional DUBA mutants, which have significantly altered dynamic properties, using the pulse sequence presented here, will allow more precise characterization of the effects of mutations on the H-bond network by providing information on arginine side chains in addition to backbone amides. The studies on arginine side chains can shed light on the mechanisms by which motions are coupled across nearly the entire enzyme molecule and facilitate the rational design of enzymes that possess desired dynamic properties, e.g., coupling of motions between functionally important elements. One of the challenges in studying DUBA dynamics is that the highly dynamic substrate binding interface, including the active site, is mostly not visible in amide-detected experiments.[20] Development of more sophisticated NMR methods, such as those employing direct ^{13}C detection,[44] will likely be needed to observe the arginines and other charged or polar side chains crucial for controlling the global dynamics. The current study does not provide additional information on the α6 helix that harbors the two charged residues, R272 and K273, which are essential for both DUBA function and for maintaining the coupled motions. Nevertheless, the easy implementation of the ^1H CPMG experiment presented here makes it an ideal choice for the rapid characterization of μs−ms motions in arginine side chains without the need to perform two separate experiments on backbone amides and arginine side-chain N^ϵ−H^ϵ. The dynamic parameters obtained from this simple experiment will be useful for comparison and benchmarking of the measurements that can be made using more sophisticated methods.

■ ASSOCIATED CONTENT

Supporting Information

The Supporting Information is available free of charge at https://pubs.acs.org/doi/10.1021/acsomega.2c00492.

The Supporting Information is available free of charge. H-bond networks in the crystal structure of DUBA (Table S1) and H-bond networks identified by ProteinTools (Figure S1) (PDF)

Accession Codes

Deubiquitinase A/OTUD5 (*Homo sapiens*), UniProtKB Q96G74.

■ AUTHOR INFORMATION

Corresponding Author

Ying Li − *Department of Chemistry, University of Louisville, Louisville, Kentucky 40208, United States;* orcid.org/0000-0001-7678-9405; Phone: (502)852-5975.; Email: ying.li.1@louisville.edu; Fax: (502)852-8149

Authors

Ashish Kabra − *Department of Chemistry, University of Louisville, Louisville, Kentucky 40208, United States*

Efsita Rumpa − *Department of Chemistry, University of Louisville, Louisville, Kentucky 40208, United States*

Complete contact information is available at: https://pubs.acs.org/10.1021/acsomega.2c00492

Funding

This work was supported by the National Institutes of Health grant R15GM123391.

Notes

The authors declare no competing financial interest.

■ ABBREVIATIONS USED

μM, micromolar; μs−ms, microsecond-to-millisecond; μs, microsecond; AMC, amino-4-methylcoumarin; CPMG, Carr−Purcell−Meiboom−Gill; DUBA, deubiquitinase A;

https://doi.org/10.1021/acsomega.2c00492
ACS Omega 2022, 7, 9936−9943

DUB, deubiquitinase; HSQC, heteronuclear single-quantum coherence; NMR, nuclear magnetic resonance; OTU, ovarian tumor; PTMs, posttranslation modifications; TROSY, transverse relaxation optimized spectroscopy

REFERENCES

(1) Clague, M. J.; Barsukov, I.; Coulson, J. M.; Liu, H.; Rigden, D. J.; Urbe, S. Deubiquitylases from genes to organism. *Physiol. Rev.* **2013**, *93*, 1289−1315.

(2) Reyes-Turcu, F. E.; Ventii, K. H.; Wilkinson, K. D. Regulation and cellular roles of ubiquitin-specific deubiquitinating enzymes. *Annu. Rev. Biochem.* **2009**, *78*, 363−397.

(3) Akutsu, M.; Dikic, I.; Bremm, A. Ubiquitin chain diversity at a glance. *J. Cell Sci.* **2016**, *129*, 875−880.

(4) Mevissen, T. E. T.; Komander, D. Mechanisms of deubiquitinase specificity and regulation. *Annu. Rev. Biochem.* **2017**, *86*, 159−192.

(5) Kayagaki, N.; Phung, Q.; Chan, S.; Chaudhari, R.; Quan, C.; O'Rourke, K. M.; Eby, M.; Pietras, E.; Cheng, G.; Bazan, J. F.; Zhang, Z.; Arnott, D.; Dixit, V. M. DUBA: a deubiquitinase that regulates type I interferon production. *Science* **2007**, *318*, 1628−1632.

(6) Rutz, S.; Kayagaki, N.; Phung, Q. T.; Eidenschenk, C.; Noubade, R.; Wang, X.; Lesch, J.; Lu, R.; Newton, K.; Huang, O. W.; Cochran, A. G.; Vasser, M.; Fauber, B. P.; DeVoss, J.; Webster, J.; Diehl, L.; Modrusan, Z.; Kirkpatrick, D. S.; Lill, J. R.; Ouyang, W.; Dixit, V. M. Deubiquitinase DUBA is a post-translational brake on interleukin-17 production in T cells. *Nature* **2015**, *518*, 417−421.

(7) González-Navajas, J. M.; Law, J.; Nguyen, K. P.; Bhargava, M.; Corr, M. P.; Varki, N.; Eckmann, L.; Hoffman, H. M.; Lee, J.; Raz, E. Interleukin 1 receptor signaling regulates DUBA expression and facilitates Toll-like receptor 9-driven antiinflammatory cytokine production. *J. Exp. Med.* **2010**, *207*, 2799−2807.

(8) Beck, D. B.; Basar, M. A.; Asmar, A. J.; Thompson, J. J.; Oda, H.; Uehara, D. T.; Saida, K.; Pajusalu, S.; Talvik, I.; D'Souza, P.; Bodurtha, J.; Mu, W.; Barañano, K. W.; Miyake, N.; Wang, R.; Kempers, M.; Tamada, T.; Nishimura, Y.; Okada, S.; Kosho, T.; Dale, R.; Mitra, A.; Macnamara, E.; Matsumoto, N.; Inazawa, J.; Walkiewicz, M.; Õunap, K.; Tifft, C. J.; Aksentijevich, I.; Kastner, D. L.; Rocha, P. P.; Werner, A. Linkage-specific deubiquitylation by OTUD5 defines an embryonic pathway intolerant to genomic variation. *Sci. Adv.* **2021**, *7*, No. eabe2116.

(9) de Vivo, A.; Sanchez, A.; Yegres, J.; Kim, J.; Emly, S.; Kee, Y. The OTUD5-UBR5 complex regulates FACT-mediated transcription at damaged chromatin. *Nucleic Acids Res.* **2019**, *47*, 729−746.

(10) Li, F.; Sun, Q.; Liu, K.; Zhang, L.; Lin, N.; You, K.; Liu, M.; Kon, N.; Tian, F.; Mao, Z.; Li, T.; Tong, T.; Qin, J.; Gu, W.; Li, D.; Zhao, W. OTUD5 cooperates with TRIM25 in transcriptional regulation and tumor progression via deubiquitination activity. *Nat. Commun.* **2020**, *11*, No. 4184.

(11) Huang, O. W.; Ma, X.; Yin, J.; Flinders, J.; Maurer, T.; Kayagaki, N.; Phung, Q.; Bosanac, I.; Arnott, D.; Dixit, V. M.; Hymowitz, S. G.; Starovasnik, M. A.; Cochran, A. G. Phosphorylation-dependent activity of the deubiquitinase DUBA. *Nat. Struct. Mol. Biol.* **2012**, *19*, 171−175.

(12) Mevissen, T. E.; Hospenthal, M. K.; Geurink, P. P.; Elliott, P. R.; Akutsu, M.; Arnaudo, N.; Ekkebus, R.; Kulathu, Y.; Wauer, T.; El Oualid, F.; Freund, S. M.; Ovaa, H.; Komander, D. OTU deubiquitinases reveal mechanisms of linkage specificity and enable ubiquitin chain restriction analysis. *Cell* **2013**, *154*, 169−184.

(13) Sahtoe, D. D.; Sixma, T. K. Layers of DUB regulation. *Trends Biochem. Sci.* **2015**, *40*, 456−467.

(14) Heideker, J.; Wertz, I. E. DUBs, the regulation of cell identity and disease. *Biochem. J.* **2015**, *465*, 1−26.

(15) Schauer, N. J.; Magin, R. S.; Liu, X.; Doherty, L. M.; Buhrlage, S. J. Advances in discovering deubiquitinating enzyme (DUB) inhibitors. *J. Med. Chem.* **2020**, *63*, 2731−2750.

(16) Dambacher, C. M.; Worden, E. J.; Herzik, M. A.; Martin, A.; Lander, G. C. Atomic structure of the 26S proteasome lid reveals the mechanism of deubiquitinase inhibition. *eLife* **2016**, *5*, No. e13027.

(17) Kim, R. Q.; Sixma, T. K. Regulation of USP7: A High Incidence of E3 Complexes. *J. Mol. Biol.* **2017**, *429*, 3395−3408.

(18) Özen, A.; Rouge, L.; Bashore, C.; Hearn, B. R.; Skelton, N. J.; Dueber, E. C. Selectively modulating conformational states of USP7 catalytic domain for activation. *Structure* **2018**, *26*, 72−84.

(19) Mevissen, T. E. T.; Kulathu, Y.; Mulder, M. P. C.; Geurink, P. P.; Maslen, S. L.; Gersch, M.; Elliott, P. R.; Burke, J. E.; van Tol, B. D. M.; Akutsu, M.; Oualid, F. E.; Kawasaki, M.; Freund, S. M. V.; Ovaa, H.; Komander, D. Molecular basis of Lys11-polyubiquitin specificity in the deubiquitinase Cezanne. *Nature* **2016**, *538*, 402−405.

(20) Kabra, A.; Li, Y. Conformational dynamics of deubiquitinase A and functional implications. *Biochemistry* **2021**, *60*, 201−209.

(21) Kabra, A.; Rumpa, E.; Li, Y. Modulation of conformational equilibrium by phosphorylation underlies the activation of deubiquitinase A. *J. Biol. Chem.* **2020**, *295*, 3945−3951.

(22) Kabra, A.; Benson, C. A.; Li, Y. Backbone ^{1}H, ^{13}C, ^{15}N resonance assignments of deubiquitinase A in non-phosphorylated and phosphorylated forms. *Biomol. NMR Assign.* **2019**, *13*, 37−42.

(23) Delaglio, F.; Grzesiek, S.; Vuister, G. W.; Zhu, G.; Pfeifer, J.; Bax, A. NMRPipe: a multidimensional spectral processing system based on UNIX pipes. *J. Biomol. NMR* **1995**, *6*, 277−293.

(24) Lee, W.; Tonelli, M.; Markley, J. L. NMRFAM-SPARKY: enhanced software for biomolecular NMR spectroscopy. *Bioinformatics* **2015**, *31*, 1325−1327.

(25) Niklasson, M.; Otten, R.; Ahlner, A.; Andresen, C.; Schlagnitweit, J.; Petzold, K.; Lundstrom, P. Comprehensive analysis of NMR data using advanced line shape fitting. *J. Biomol. NMR* **2017**, *69*, 93−99.

(26) Ahlner, A.; Carlsson, M.; Jonsson, B. H.; Lundstrom, P. PINT: a software for integration of peak volumes and extraction of relaxation rates. *J. Biomol. NMR* **2013**, *56*, 191−202.

(27) O'Connell, N. E.; Grey, M. J.; Tang, Y.; Kosuri, P.; Miloushev, V. Z.; Raleigh, D. P.; Palmer, A. G., 3rd Partially folded equilibrium intermediate of the villin headpiece HP67 defined by ^{13}C relaxation dispersion. *J. Biomol. NMR* **2009**, *45*, 85−98.

(28) Abramovich, D.; Vega, S. Derivation of broadband and narrowband excitation pulses using the Floquet formalism. *J. Magn. Reson. A* **1993**, *105*, 30−48.

(29) Iwahara, J.; Clore, G. M. Sensitivity improvement for correlations involving arginine side-chain Nε/Hε resonances in multi-dimensional NMR experiments using broadband ^{15}N 180° pulses. *J. Biomol. NMR* **2006**, *36*, 251−257.

(30) Li, Y.; Altorelli, N. L.; Bahna, F.; Honig, B.; Shapiro, L.; Palmer, A. G., 3rd Mechanism of E-cadherin dimerization probed by NMR relaxation dispersion. *Proc. Natl. Acad. Sci. U. S. A.* **2013**, *110*, 16462−16467.

(31) Kumar, G. S.; Clarkson, M. W.; Kunze, M. B. A.; Granata, D.; Wand, A. J.; Lindorff-Larsen, K.; Page, R.; Peti, W. Dynamic activation and regulation of the mitogen-activated protein kinase p38. *Proc. Natl. Acad. Sci. U.S.A* **2018**, *115*, 4655−4660.

(32) Beaumont, V. A.; Reiss, K.; Qu, Z.; Allen, B.; Batista, V. S.; Loria, J. P. Allosteric impact of the variable insert loop in Vaccinia H1-related (VHR) phosphatase. *Biochemistry* **2020**, *59*, 1896−1908.

(33) Cui, D. S.; Lipchock, J. M.; Brookner, D.; Loria, J. P. Uncovering the molecular interactions in the catalytic loop that modulate the conformational dynamics in protein tyrosine phosphatase 1B. *J. Am. Chem. Soc.* **2019**, *141*, 12634−12647.

(34) Torgeson, K. R.; Clarkson, M. W.; Kumar, G. S.; Page, R.; Peti, W. Cooperative dynamics across distinct structural elements regulate PTP1B activity. *J. Biol. Chem.* **2020**, *295*, 13829−13837.

(35) Nashine, V. C.; Hammes-Schiffer, S.; Benkovic, S. J. Coupled motions in enzyme catalysis. *Curr. Opin. Chem. Biol.* **2010**, *14*, 644−651.

(36) Henzler-Wildman, K. A.; Lei, M.; Thai, V.; Kerns, S. J.; Karplus, M.; Kern, D. A hierarchy of timescales in protein dynamics is linked to enzyme catalysis. *Nature* **2007**, *450*, 913−916.

(37) Lisi, G. P.; Loria, J. P. Using NMR spectroscopy to elucidate the role of molecular motions in enzyme function. *Prog. Nucl. Magn. Reson. Spectrosc.* **2016**, *92-93*, 1−17.

https://doi.org/10.1021/acsomega.2c00492
ACS Omega 2022, 7, 9936−9943

(38) Romero-Rivera, A.; Garcia-Borràs, M.; Osuna, S. Role of conformational dynamics in the evolution of retro-aldolase activity. *ACS Catal.* **2017**, *7*, 8524−8532.
(39) Donald, J. E.; Kulp, D. W.; Degrado, W. F. Salt bridges: Geometrically specific, designable interactions. *Proteins: Struct. Funct. Genet.* **2011**, *79*, 898−915.
(40) Trbovic, N.; Cho, J. H.; Abel, R.; Friesner, R. A.; Rance, M.; Palmer, A. G., 3rd Protein side-chain dynamics and residual conformational entropy. *J. Am. Chem. Soc.* **2009**, *131*, 615−622.
(41) Werbeck, N. D.; Kirkpatrick, J.; Hansen, D. F. Probing arginine side-chains and their dynamics with carbon-detected NMR spectroscopy: application to the 42 kDa human histone deacetylase 8 at high pH. *Angew. Chem., Int. Ed.* **2013**, *52*, 3145−3147.
(42) Esadze, A.; Chen, C.; Zandarashvili, L.; Roy, S.; Pettitt, B. M.; Iwahara, J. Changes in conformational dynamics of basic side chains upon protein-DNA association. *Nucleic Acids Res.* **2016**, *44*, 6961−6970.
(43) Nguyen, D.; Hoffpauir, Z. A.; Iwahara, J. Internal motions of basic side chains of the Antennapedia homeodomain in the free and DNA-bound states. *Biochemistry* **2017**, *56*, 5866−5869.
(44) Pritchard, R. B.; Hansen, D. F. Characterising side chains in large proteins by protonless ^{13}C-detected NMR spectroscopy. *Nat. Commun.* **2019**, *10*, No. 1747.
(45) Karunanithy, G.; Shukla, V. K.; Hansen, D. F. Methodological advancements for characterising protein side chains by NMR spectroscopy. *Curr. Opin. Struct. Biol.* **2021**, *70*, 61−69.

https://doi.org/10.1021/acsomega.2c00492
ACS Omega 2022, 7, 9936−9943